Journal of Marine Research, 41, 511–538, 1983

Modelling the advection of vertically migrating shrimp larvae

by Peter C. Rothlisberg[1], John A. Church[2] and Andrew M. G. Forbes[2]

ABSTRACT

The role of larval advection in determining the complex, large–scale patterns of immigration of penaeid postlarvae in the Gulf of Carpentaria is investigated by modelling the interaction between diurnal vertical migration of larvae with wind-forced and tidal currents. Eight vertical migration schemes are modelled in which both the timing of the migration and the position of the larvae in the water column are varied. These schemes are then coupled with both two-dimensional and three-dimensional models of the currents of the Gulf, to examine horizontal advection of larvae. When the larvae migrate vertically with a diurnal period, their horizontal advection is enhanced. The largest horizontal advection distances occur when the larvae move diurnally from the water column into the bottom boundary layer. Advection distances of up to 165 km are possible during the two to three week planktonic larval period. This distance corresponds to, and may determine, the offshore extent of the adult distribution. The onshore advection pattern of larvae varies in both space and time (on a seasonal scale) and is consistent with the observed spatial and temporal recruitment patterns seen by sampling postlarval immigation into nursery areas. During the period of highest reproductive activity (March) in the southeastern corner of the Gulf, the area of the largest fishery, the advection of larvae is offshore and little recruitment of postlarvae to the nursery grounds is accomplished. Six months later, during the next period of reproductive activity (October), when the number of spawning female shrimp is much lower, the phase of the tidal currents, relative to the day-night cycle, has progressed 180° and the larvae are moved onshore allowing postlarvae access to their estuarine nursery grounds several months prior to the main fishing season (March).

1. Introduction

Hjort (1914) was the first to suggest that the survival of the early life history stages was important in establishing year-class strength of species with pelagic larvae. He considered that there were two factors (one biotic, one abiotic) of particular importance viz: food availability at the time of first feeding, and suitability of currents to take the larvae from the spawning grounds to habitats required for the next stage of the life cycle. The importance of the presence of adequate food for larvae at specific times in the early life history, not just first feeding, has been called the 'critical period

1. Division of Fisheries Research, CSIRO Marine Laboratories, P.O. Box 120, Cleveland, Qld 4163, Australia.
2. Division of Oceanography, CSIRO Marine Laboratories, P.O. Box 1538, Hobart, Tas. 7001, Australia.

concept' and has been studied widely, geographically and taxonomically in both the laboratory and the field (for reviews see Marr, 1956; May, 1974).

Marine larval advective and diffusive studies to date have been largely descriptive, speculative or correlative, with little data on the mechanisms required for larval transport (Rae, 1957; Bakken, 1966; Wickett, 1967; Hart, 1975). The surface currents are often only vaguely known by returns of drift bottles and surface drogues, (Colton and Temple, 1961; Saville, 1965; Dragesund, 1970) or only in the broadest terms with limited seasonal, vertical or small-scale resolution (Parrish *et al.*, 1981).

Understanding of the advective processes affecting larval movement is further complicated if the larvae undergo diurnal, tidal or ontogenetic vertical migration (Graham *et al.*, 1972; Strathmann, 1974; Okubo, 1980). Hardy (1935) was the first to suggest that vertical migration through a variable current field could affect horizontal displacement. He also considered that in this way animals avoided prolonged contact with unfavorable environments and this saltatory movement gave rise to patchiness. The patchiness part of his hypothesis has been studied (Miller, 1970; Kamykowski, 1974, 1976; Riley, 1976) but the effect of vertical migration on advection and diffusion is largely untested. Nevertheless, this mechanism has been invoked to aid maintenance of position within estuaries (Bousefield, 1955; Pearcy, 1962; Weinstein *et al.*, 1980; Wooldridge and Erasmus, 1980) and on continental shelves (Walford, 1938; Wroblewski, 1982) or alternatively to enhance horizontal displacement up an estuary (Carriker, 1951; Wood and Hargis, 1971; Sandifer, 1975; Sulkin *et al.*, 1980), alongshore (Longhurst, 1976; Efford, 1970) or onshore (Woodmansee, 1966; Penn, 1975; Phillips *et al.*, 1979) often against prevailing currents. In no instance however, have these mechanisms been demonstrated by monitoring both the vertical behavior and the *in situ* current regimes simultaneously.

The distance, direction and timing of larval movement are of particular importance to species whose spawning grounds are separate and some distance from their nursery grounds (Istock, 1967; Cushing and Harden Jones, 1968; Dragesund, 1970; Paulik, 1973). Estuarine-marine dependency is very common among species that support major vertebrate and invertebrate fisheries (Gunter, 1980), and a large number of penaeid shrimp (prawn) genera have offshore spawning grounds and nearshore or estuarine nursery ground requirements for postlarvae or juveniles (for review see Garcia and Le Reste, 1981).

Previous descriptive studies of vertical migration of early penaeid larvae (Racek, 1959; Eldred *et al.*, 1965; Temple and Fischer, 1965; Jones *et al.*, 1970) have been contradictory and have shed little light on a possible mechanism for onshore transport. Penn (1975) hypothesized, based on an idealized larval behavior and limited knowledge of current regimes, that larval *Penaeus latisulcatus* in Western Australia used day-night differences in speed and direction of tidal currents on the surface and bottom to move onshore during certain times of the year. Rothlisberg (1982) showed that the extent of vertical migration changed as penaeid larvae developed and that the behavior

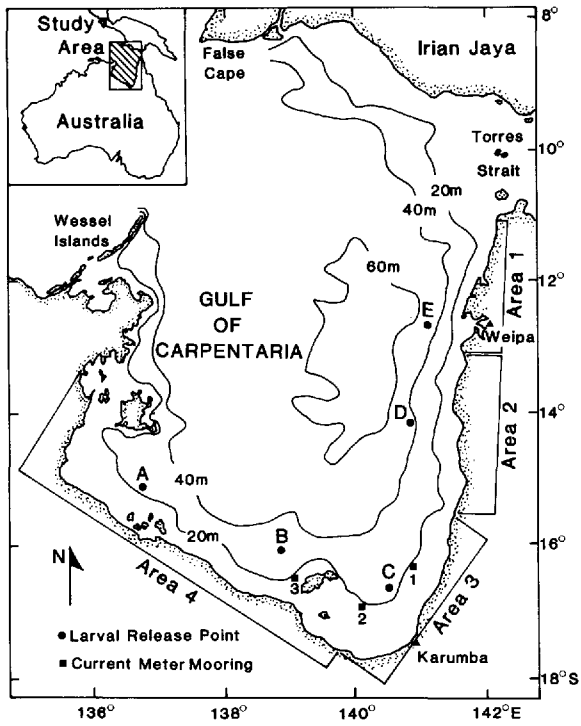

Figure 1. Map of the Gulf of Carpentaria and Arafura Sea encompassed in the current study. Areas 1–4 refer to Staples' (1979) postlarval recruitment patterns (see text). Points A–E are larval release points used by the models. Points 1–3 are sites of current meters used for model verification.

of all larval stages was mediated by light penetration. Further, by simultaneously measuring current speed and direction at depth along with the larval shrimp vertical distribution, the distance and direction of larval shrimp movement was approximated by extrapolating from the short-term (24 h) sampling to the 7–14 day planktonic period. From this limited sampling the importance of the vertical position in the water column in determining the resultant advection distance and direction was shown. However, because the study was localized and short-term it was not very useful in explaining the large-scale temporal and spatial patterns of recruitment recently described for postlarval *P. merguiensis* in the Gulf of Carpentaria (Staples, 1979).

Staples (1979) delineated four areas in the Gulf of Carpentaria with characteristic patterns of postlarval immigration into estuarine nursery grounds (Fig. 1). Area 1, in the northeastern Gulf, has recruitment from February to June with a peak in March–April. Area 2, in the middle of the east coast, has year-round recruitment. Area 3, in the southeastern Gulf, has recruitment from October to June with a peak in November–December, five months out of phase with Area 1. Area 4, covering the

southwestern side of the Gulf, has year-round recruitment as well, but only very intermittantly with rivers often not having any recruitment for several years. As there are two spawning periods of *P. merguiensis* in the Gulf (October–December and March–May; Crocos and Kerr, 1983) in Area 1 the March–May larvae survive and in Area 3 the October–December larvae survive. Random diffusion of larvae cannot explain the seasonal changes in larval transport that may be responsible for the loss of the larvae from the March–May spawning in the southern Gulf and the October–December spawning in the northern Gulf.

A knowledge of the circulation in the Gulf is essential. Early studies of the hydrological conditions in the Gulf of Carpentaria were completed by Rochford (1966) and Newell (1973). While Newell (1973) inferred large-scale baroclinic motion, current meter records (Cresswell, 1971; Church and Forbes, 1983) indicate that barotropic tide and wind-induced currents are dominant. Reinecker (1979), Webb (1981) and Church and Forbes (1981) developed two-dimensional (depth-averaged) models of the tidal circulation. In the area of the Gulf considered here, the diurnal tidal constituents (K_1 and O_1) are dominant and the semi-diurnal constituents (M_2 and S_2) are small. Further north near the coast of Irian Jaya the semi-diurnal constituents are much larger. Forbes and Church (1983) produced models of the mean circulation (induced by nonlinear tidal effects, seasonal winds and baroclinic effects) and found good agreement with the tracks of free-drifting satellite-tracked buoys.

Of these studies, only those which developed numerical models have enough spatial and temporal resolution to allow any meaningful evaluation of the role of the currents in explaining larval advection and survival. Unfortunately these models do not contain any information on the vertical current structure whereas the results of Rothlisberg (1982) have shown the importance of diurnal vertical migration of the larvae.

Section 2 (and the Appendix) of this paper describe an Ekman dynamics model which gives the vertical structure of the currents resulting from surface and bottom stresses as well as from pressure gradients. We then treat the shrimp larvae as tracers which move vertically through the water column, simulating the range of larval behaviors discussed by Rothlisberg (1982), in Section 3. The interaction between the larval behavior and the physical environment is treated in Section 4 and the resultant patterns of larval advection are presented in Section 5. These results are then discussed (Section 6) in an attempt to explain the disagreement between the timing and size of observed recruitment of *P. merguiensis* larvae into the estuarine nursery areas and the timing of the two spawning peaks. We also attempt in Section 6 to explain the temporal variation of the recruitment of larvae into the two most closely studied regions of the Gulf (Areas 1 and 3 in Fig. 1).

2. Models of current structure

The two-dimensional, depth-averaged model of Church and Forbes (1981) and Forbes and Church (1983) determined the barotropic tidal and wind-forced currents of

the Gulf of Carpentaria by solving the equations of continuity and conservation of momentum (including the nonlinear terms and quadratic bottom friction) by an alternating-direction, semi-implicit finite-difference technique (Leendertse, 1967). The area considered in their model included all the Gulf north to Irian Jaya and from Torres Strait in the east to a line joining Wessel Islands to False Cape in the west. A square grid (grid length, 27.8 km) aligned 19° east of north was used to overlay the area giving 25 × 37 arrays for the variables. The smooth bathymetry means that the grid can resolve most of the major bathymetric features. On the open boundary, between the Wessel Islands and False Cape, tidal elevations were specified. The tidal flow through Torres Strait (estimated from tidal constants at each end of the channel) was also specified as a boundary condition.

Frictional effects both at the surface and at the bottom lead to significant departures from the vertical averaged currents. The Ekman depth (the depth of frictional influence) δ_E is

$$\delta_E = \left(\frac{\nu}{2f}\right)^{1/2} \tag{2.1}$$

where f is the Coriolis parameter (which is a function of latitude) and for the vertical eddy viscosity ν, we use the Bowden *et al.* (1959) result

$$\nu = 2.5 \times 10^{-3}\, h\,|u|. \tag{2.2}$$

For a depth h of 30 m and a velocity $|u|$ of 0.4 m s^{-1}, the Ekman depth at a latitude of 15S is 20 m. Thus we expect all of the water column to be affected by bottom and surface stress and in fact, the bottom and surface Ekman layers overlap.

The velocity profile is intimately related to the vertical variation of the viscosity ν. Unfortunately, there are few data available which give detailed information on the variation of ν through the water column and there have been few detailed verifications of three-dimensional models. The data of Bowden *et al.* (1959) indicate a mid-depth maximum for ν and it is generally thought that ν decreases rapidly near the boundaries. Tee (1979, 1982) found that if he assumed ν constant throughout the water column (i.e., right to the boundaries), he could not reproduce the observed velocity structure. If however, a sub-layer model in which ν became small near the lower boundary was used, the observed velocity structure could be modelled (within the accuracy of the measurements) independent of the detailed form of ν in the rest of the water column.

Here, we will assume the velocity is driven by the surface pressure gradient, determined from the two-dimensional model of Church and Forbes (1981), Forbes and Church (1983), and surface wind stress, and assume that a logarithmic sub-layer exists. Rather than modelling this layer explicitly, we will assume linear friction at the top of this layer h^+; i.e., for a complex velocity $w = u + iv$ (where u and v are the two velocity components and $i = \sqrt{-1}$)

$$\nu \frac{\partial w}{\partial z}\bigg|_{z=-h^+} = bw \tag{2.3}$$

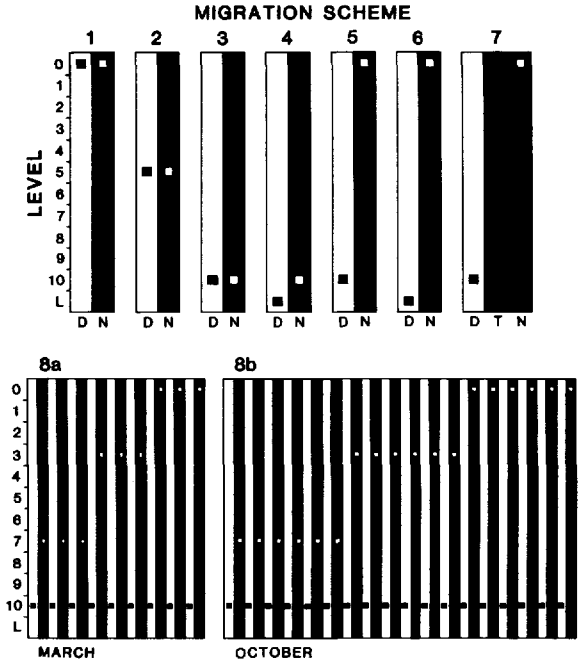

Figure 2. Schematic representation of larval vertical distribution patterns during day (D), night (N) and transitional (T) periods of dawn and dusk. Depth levels are explained in the text. ⊡ = day level: ■ = night level.

where b is the linear friction coefficient, z is the vertical axis, and we use constant viscosity given by Eq. 2.2 in the rest of the water column. In the technique which uses the analytical solution of Jordon and Baker (1980) (see the Appendix for details), we neglect all nonlinear terms and its thus impossible to reproduce accurately the second order tide-induced residual currents. The solution used is dependent on the nondimensional number $K = bh/\nu \approx 1$ and the exact value of K was chosen by comparing the results for u and v with the observations of Church and Forbes (1983).

3. Vertical migration patterns

Eight vertical migration schemes were formulated, based on behavior patterns seen in the field (Rothlisberg, 1982) plus some extreme situations for comparison (Fig. 2). The water column, regardless of depth, was divided into tenths; level 0 represents the surface, level 5 mid-depth, level 10 the bottom of the calculated Ekman current profile where there is a finite velocity, and level L the logarithmic layer. If the larvae entered the logarithmic layer it was assumed they were close enough to the bottom so that they would be in a near-zero velocity field.

The eight schemes of larval shrimp migration are numbered with increasing complexity (Fig. 2). Schemes 1, 2 and 3 represent nonmigrating larvae with the larvae

spending all of their time at either the surface, mid-depth or near-bottom (level 10) respectively. Scheme 4 has the larvae within the logarithmic layer by day and moving just up into the water column (level 10) at night. In scheme 5 the larvae move from the near-bottom (level 10) by day to the surface at night and in scheme 6 the larvae move from level L by day to the surface by night. Schemes 7 and 8 have stepped migratory patterns. In scheme 7 larvae spend the day at level 10 and move to the surface at night, with the larvae spending 1 h at each of two transitional depths during both the ascent and descent. Finally, scheme 8 simulates the developing larvae's increasing capacity for vertical migration as seen in the study of Rothlisberg (1982). The larvae progress through three planktonic stages each with several substages. The three zoeal substages move only within the lower one third of the water column, the three mysis substages move through the lower two thirds of the water column and the postlarvae move throughout the entire water column. The postlarva goes through an indeterminate number of molts before becoming benthic in the nursery grounds. In scheme 8a, in March, with relatively warm water temperatures, the larvae spend one day in each larval substage, thus from the seventh day onward larvae move throughout the whole water column. In October, when water temperatures are lower, each larval substage was assumed to last 2 days, thus from day 13 onward larvae migrate through the whole water column. The larval growth rates are based on experimental larval rearing studies (Mock and Murphy, 1970; Rothlisberg, unpublished data).

As the modelled larvae were advected into shallower water, a nonmigrator which started at 20 m in 40 m total depth (level 5) would be at 10 m in 20 m of water and at 5 m in 10 m of water (still level 5). Since the larvae's ability to migrate vertically is defined here by depth fraction, not as an absolute distance (an assumption that simplifies calculations), the levels they can reach will be effectively nearer the surface in shallower water than in deep water.

4. The larval advection models

Staples (1979) suggested that the Weipa and the Karumba areas had marked peaks in recruitment in April and November respectively. We therefore chose to model the advection of vertically migrating larvae in the months of March (March 6, 1978, was the exact date chosen for the start of the simulation) and October (October 10, 1978) at two locations (C and E, Fig. 1). These two locations were chosen for their proximity to Staples' recruitment areas and because of their high probability for penaeid spawning based on adult distributions (Lucas *et al.*, 1979) and reproductive activity (Crocos and Kerr, 1983).

The two-dimensional model was run for 20 days commencing at the above two dates (plus a suitable spin up time before these dates for the decay of initial transients). The four principal tidal constituents (K_1, O_1, M_2 and S_2) were included and for the October period two runs were made, one with mean winds (Forbes and Church, 1983) and one without. In March, the mean winds were light and were not included. The surface

elevations resulting from these model runs were then combined with the Ekman model (Appendix Eq. 14) and the vertical structure of the horizontal currents determined at the location of the model larvae. These currents were then used to advect the larvae using a single step time-centered scheme. In the present case where there is smooth bathymetry, only a slow spatial change in the tidal character, and slow horizontal movement of the larvae, the difference between computing the three-dimensional current structure on an Eulerian grid and interpolating to the larvae, and computing the current structure in a Lagrangian manner, is negligible.

In addition to using the three-dimensional current structure for computing the advection of the larvae, we also used directly the currents computed with the two-dimensional model. The velocities of the larvae were obtained by bi-linearly interpolating ($f = a + bx + cy + dxy$) from the velocities at the surrounding 4 grid points. In this scheme, the larvae were considered to be either in the water column when they were advected with the ambient current or close to the bottom and assumed stationary. This simple alternative was included to determine whether approximate results, which could be determined more quickly and more cheaply with the two-dimensional model, would be useful as general indicators of advective trends.

5. Results

Vertical current structure

The vertical current structure was evaluated for three values (0.5, 1, 2) of the nondimensional number $K = bh/\nu$. The decrease in velocity with increasing depth observed in the current meter observations of Church and Forbes (1983) was used to discriminate between the solutions. At current meter location 2 (Fig. 1), the ratio of the K_1 amplitudes seen in recordings of current meters moored at 6 and 11 m below the surface (water depth 17 m) was 0.84 and 0.86 (north and east components respectively) and for the O_1 constituent the values were 0.85 and 0.65. The model results near this site gave 0.83 and 0.78 for $K = 2$, 0.89 and 0.86 for $K = 1$ and 0.94 and 0.94 for $K = 0.5$. Although both $K = 1$ and $K = 2$ appear to yield similar fits ($K = 1$ marginally better) to the above ratios, $K = 1$ produces velocities that are too large when compared with the two-dimensional depth-averaged model. $K = 2$ is, overall, the best fit, and this value was used in all of the computations. The surface and bottom velocities (at current meter location 2) computed with the three-dimensional model (Appendix Eq. A14) are compared with the results of the two-dimensional depth-averaged model in Figure 3. Fourteen hours after the summation commenced the surface and the bottom velocities encompassed the two-dimensional depth-averaged velocities.

Analysis of the results indicated that the maximum difference between surface and bottom velocities occurs at times of peak flow. A typical hodograph of the current structure for both the wind and no wind situation at peak flow is shown in Figure 4 for

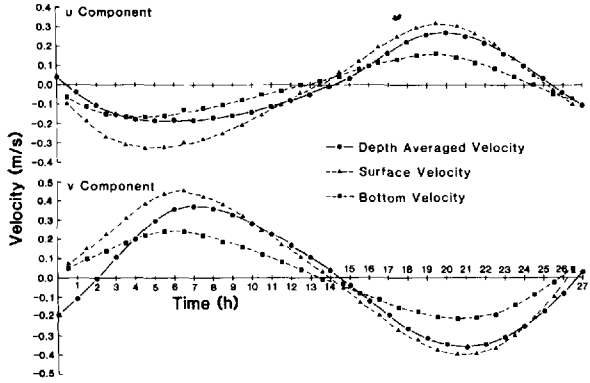

Figure 3. Comparison of modelled current velocity components at current meter location 2 (u-eastward, v-northward) generated by the two-dimensional, depth-averaged, and three-dimensional models.

two water depths (39 and 49 m) near release point E. In both cases there is little change in direction of the current with depth but the speed increases by a factor of two from the bottom to the surface. Similar small variations in direction and large variations in speed occurred at the other locations and depths. Near the change of the tide, however, there were significant changes in the direction with depth (Fig. 5). The maximum variation in direction with depth was 44° at 39 h in 41 m of water. As the depth decreased, the maximum variation in direction of the current decreased to 17° at 40 h in water of 20 m depth and only 4° at 39 h in water of 11 m depth. It was clear that the modelled Ekman veering effects decreased with decreasing water depth, and that in shallow water there was no significant difference in current direction from surface to bottom throughout the tidal cycle.

With wind applied to the model, profiles do not differ significantly from the nonwind case. The surface current is, as expected, more affected by the wind than the bottom current as shown in Figure 4. For a water depth of 39 m, the surface current near release point E differs by 10% in speed, between wind and nonwind cases. In the deeper water, 49 m, there is a current direction difference, due to the wind, of 4° at the surface, but 0° at the bottom.

In Figure 5, again the greatest difference in current direction, between the wind and nonwind cases is at the surface although at this location in the southern part of the Gulf (near release point C) the applied wind stress for October is about 1/10 of the wind stress in the northern part of the Gulf, so the effect on the current profiles is proportionately less.

Larval advection patterns

a. Spatial. The positions of the larvae relative to the starting locations near Karumba and Weipa for the March period are plotted at 5-day intervals for the three-

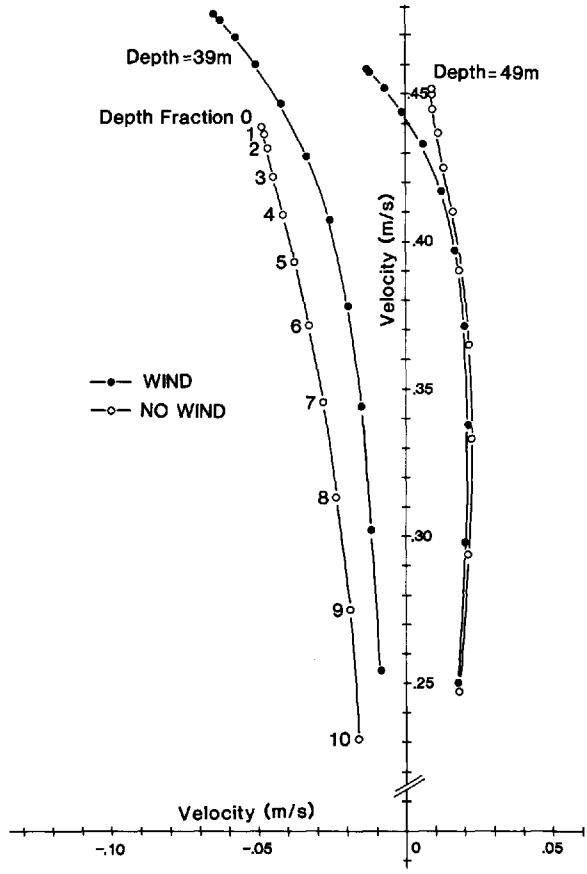

Figure 4. Hodograph (line joining tips of vectors representing current speeds at 10 depth intervals from surface to bottom) of current structure at two depths (39 and 49 m) near release point E (see Fig. 1), for both wind and nonwind situation at time of peak flow (model time = 32 h).

dimensional current model and are presented in Figure 6A and 6B. Also shown are the positions of the larvae after 20 days when the two-dimensional depth-averaged currents were used for migration schemes 1 and 6. The most significant difference in advection is between the larvae which do not migrate vertically (schemes 1–3) and those which migrate (schemes 4–8). Near Karumba, the nonmigrators are advected only short distances (Fig. 6A), 20 km northwest for the three-dimensional model and approximately 10 km southwest for the depth-averaged currents. The larvae which follow scheme 6 are advected north 165 km, for the other schemes they are advected about 90 km north and for the depth-averaged currents they are advected 150 km north. Near Weipa (Fig. 6B), the nonmigrators drifted 10–30 km south depending on which level they occupied. In contrast, the migrators were advected north. If the larvae

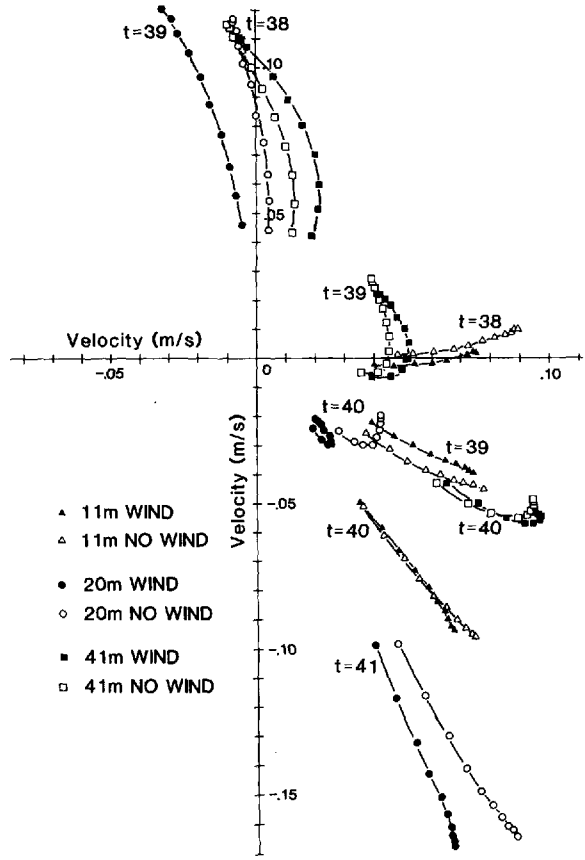

Figure 5. Hodographs of current structure at three depths (11, 20 and 41 m) near release point C (see Fig. 1) for wind and nonwind situation near the turn of the tide (model time = 38–41 h).

behave as in scheme 6, they are advected 100 km north, for the other schemes they are advected 40–50 km north and for the depth averaged currents they are advected 90 km north.

In October (no wind case), the situation is quite different (Fig. 7A, 7B). Near Karumba (Fig. 7A), the nonmigrators are advected short distances (up to 20 km north) while the migrators are advected 125 km south for scheme 6, 45–70 km south for the other schemes and 120 km south for the depth-averaged results. Near Weipa (Fig. 7B), the nonmigrators in the three-dimensional model are advected 10–15 km west and in the two-dimensional model they are advected 25 km south. The migrators that follow scheme 6 are advected 85 km south and in the other schemes are advected 30–50 km south. With depth-averaged currents they are advected about 90 km south.

When wind stress is included in the October model (Fig. 8), the only significant

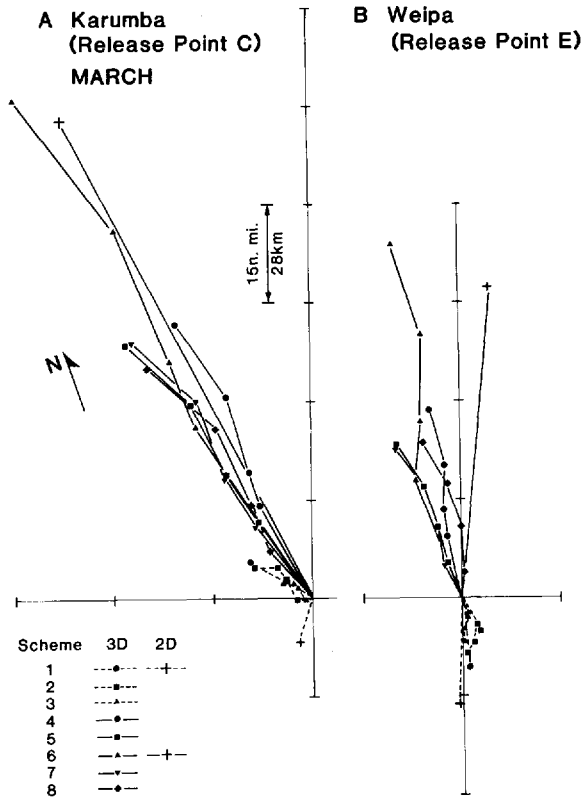

Figure 6. Modelled larval advective distances and directions in March. (A) larvae released at point C near Karumba. (B) larvae released at point E near Weipa. 3D: three-dimensional model. 2D: two-dimensional depth-averaged model. Dashed lines are nonmigratory schemes, solid lines are migratory schemes (see Fig. 2).

differences are in the Weipa area (Fig. 8B). The near-surface nonmigrators are affected the most by the southeasterly winds and are advected north or northwest distances of 20 km to 55 km. The migrators are less affected by the wind and are advected south, 85 km for scheme 6, 20–30 km for the other schemes and 60 km for the depth-averaged currents. With the three-dimensional model, the effect of wind stress results in larvae that remain near the surface with no vertical migration being advected further west while the larvae that remain near the bottom are advected slightly onshore.

To give a clearer spatial picture, the results of the two-dimensional advective patterns, without vertical migration (scheme 1) and with vertical migration when the larvae were allowed to enter level L during the day (scheme 6) for five locations, are shown in Figure 9A (October) and 9B (March). In October (Fig. 9A) the final positions without migration and without wind show a small drift (10–15 km) in the

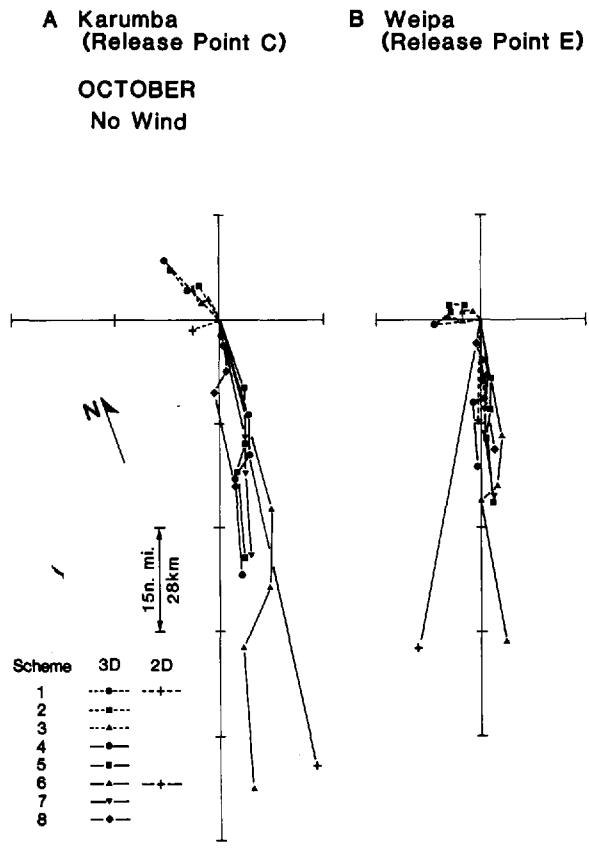

Figure 7. Modelled larval advective distances and directions in October with *no* wind stress applied to the model. (A) larvae released at point C near Karumba. (B) larvae released at point E near Weipa. 3D: three-dimensional model. 2D: two-dimensional depth-averaged model. Dashed lines are nonmigratory schemes, solid lines are migratory schemes (see Fig. 2).

direction of the residual tidal current. With vertical migration and without wind stress, the net drift increases dramatically (60–150 km), generally southward from spawning locations B, C, D and E and west at location A. For locations A, B and C this is shoreward. At the two northern spawning locations (D and E) the southward drift of the larvae is about 70 km alongshore. When October mean wind stress is applied the net drift at locations A, B and C is not significantly different. However, at locations D and E with vertical migration, the wind decreases the extent of the larval drift by about 25%. Without vertical migration the advection is reversed, with the larvae moving north by 15–50 km (locations C and D respectively) after 20 days.

The larval advection for March, for the same five potential spawning locations is shown in Figure 9B. A difference of 180° in the phase of the October and March tides,

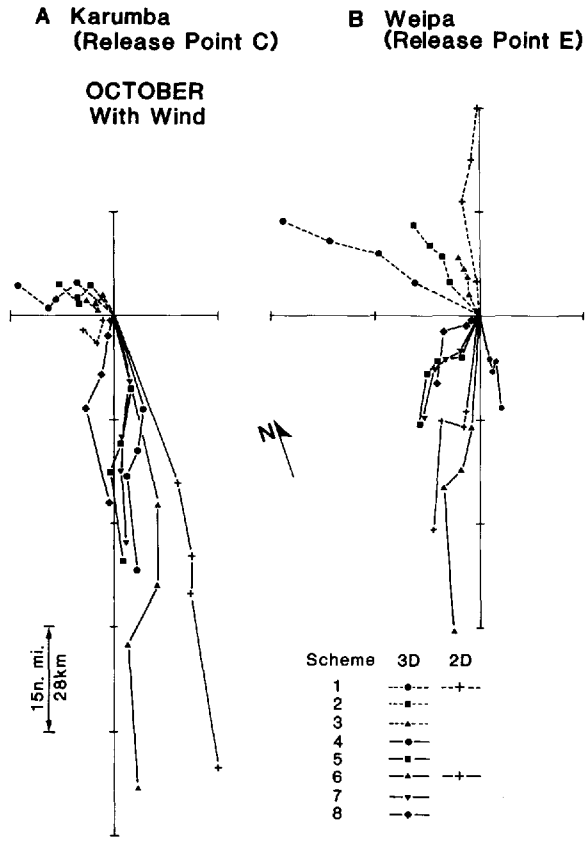

Figure 8. Modelled larval advective distances and directions in October *with* wind stress applied to the model. (A) larvae released at point C near Karumba. (B) larvae released at point E near Weipa. 3D: three-dimensional model. 2D: two-dimensional depth-averaged model. Dashed lines are nonmigratory schemes, solid lines are migratory schemes (see Fig. 2).

when combined with the fixed day-night vertical migration cycle results in drift, after 20 days, of a comparable magnitude, but in the opposite direction. At locations A, B and C the net drift is offshore, at location D alongshore to the north, and at E to the northeast. Without vertical migration, the net drift at all five locations is virtually identical with the October picture (10–15 km).

b. Temporal. The results presented so far have concentrated on advection of larvae released at two particular times, thought to coincide with the peaks of spawning activity. We would also like to know how the seasonal progression of the phase of the tide, relative to the day-night cycle, and how the spring-neap cycle, affect advection. The results of the previous section show that as long as there was some vertical migration with the day-night cycle, the direction and distance of advection of larvae in

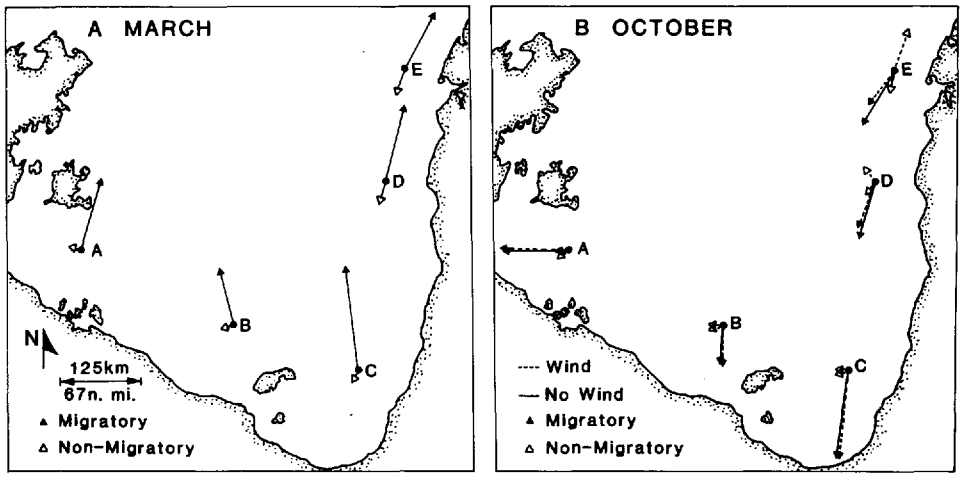

Figure 9. Spatial variation in larval advection after 20 days from the two-dimensional model at all five larval release points, for both migratory and nonmigratory larvae in, (A) March, and (B) October. Wind stress was only applied to the model in October.

each scheme were approximately the same (within a factor of about 2). Thus we can get some idea of the seasonal advection of vertically migrating larvae by evaluating an integral which we shall call the advective potential (*AP*):

$$AP = \int_{\text{day}} \mathbf{u}(t)\, f(t)\, dt,$$

where *AP* is the distance the larvae could move in one day. Here $f(t)$ is a function which scales the velocity $\mathbf{u}(t)$ according to the time of day. For simplicity, we set $f(t) = 0$ during daylight hours and $f(t) = 1$ during the night, corresponding to larvae in the logarithmic layer during the day and in the flow at night. For evaluating $\mathbf{u}(t)$, we included the four major tidal constituents (O_1, K_1, M_2 and S_2) and used the results of the model of Church and Forbes (1981) to determine the amplitude and phase of each constituent. The *AP* is an Eulerian measurement whereas the earlier results were of a Lagrangian nature. The tidal currents can now be evaluated for any time of the year at any selected station and the resultant larval advection approximated.

The results of evaluation *AP* for locations C and E for 1978 are shown in Figure 10A and 10B. Here we have used only the north-south component of $\mathbf{u}(t)$. Two periodicities are apparent. Firstly, there is a periodicity of approximately 14 days which is a combined result of the modulation of the amplitude of the current during the spring-neap cycle and of the phase of the current relative to the day-night cycle. Secondly, there is an annual cycle due to the gradual progression of the phase of the dominant K_1 tide relative to the day-night cycle. For location C, (Fig. 10A) day 325 (November 21) is approximately the last day on which vertically migrating larvae can be advected in a southward direction toward the nursery areas by the tidal currents.

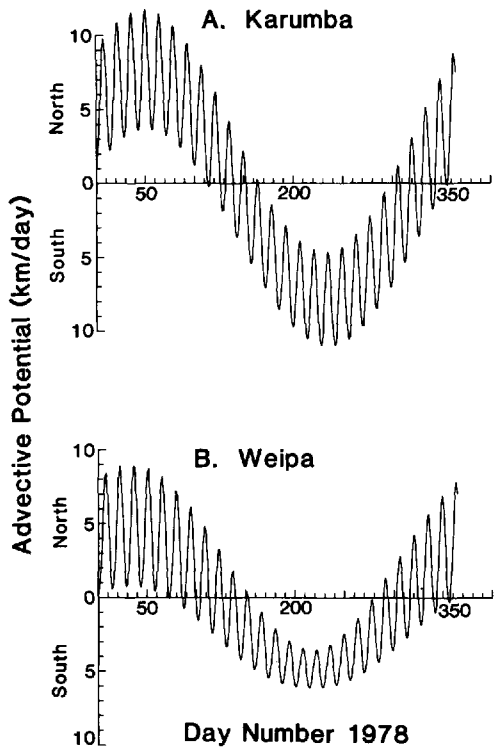

Figure 10. Temporal variation in advective potential (see text) for (A): larval release point C (near Karumba), and (B): larval release point E (near Weipa) for the calendar year 1978.

For locations closer to shore and to the mouths of rivers in the southeastern Gulf this day will be a little later. It should be noted that the determination of the last day for southward advection is sensitive to the time of day that larvae migrate vertically. Subsequent runs showed that for each hour earlier that the larvae leave the lower levels at dusk and return to the lower levels at first light, the last day for southward advection is extended by approximately 14 days. Change in the time of the vertical migration will also affect the phase of the 14-day signal.

6. Discussion

Current structure

The three-dimensional current model we developed is a hybrid of a two-dimensional depth-averaged model and a linear Ekman model which gives the vertical structure. The two-dimensional model requires a closure scheme for determining the bottom stress. A constant drag coefficient (adjusted so that the model predictions of tide height agree with the observations of tide height) combined with the depth-averaged velocity

(determined from including the four major tidal constituents) was used. Use of the near-bottom velocity would be more realistic. Johns (1978) felt this was an important criticism of depth-averaged models whereas the work of Heaps and Jones (1981) and Tee (1979, 1982) indicate that apart from an hour or so near the change of tide, the use of a depth-averaged velocity should be acceptable for well-mixed conditions when only the barotropic signal is present. The present results indicate that except at periods near the change of the tide there is little variation in direction of the current through the water column and the direction of the bottom stress would be almost independent of the velocity used in its evaluation. At the change of the tide in the deeper water there were variations in direction of the current of up to 40°. However at this time the currents are small ($\approx$0.05 m s^{-1}) and the results of the depth-averaged model should not be greatly affected by the small bottom stress. In shallower water this direction difference is smaller.

Unfortunately, in the Gulf there were only two discrete depths at which we could verify the vertical structure of the currents determined with the Ekman model. The data (Church and Forbes, 1983) show a reduction in velocity magnitude with depth at approximately the rate determined by the model. There is also little variation in direction with depth in the observations, in agreement with the model results. It was not possible to verify the structure of the wind-generated currents as there are no suitable data. This is due partly to the lack of a reliable time series of wind data over the Gulf and, in addition, the currents measured by Church and Forbes (1983) were not significantly correlated with wind data from a nearby land based meteorological station.

Larval advection

In the shallow, well-mixed Gulf of Carpentaria the vertical extent of the migration was less important than the proximity to the bottom. The advective distances and directions of all schemes in which the larvae moved into the water column at night were comparable. From the modelling it also became apparent that an epibenthic mode (where larvae settle on the bottom) during the day but rise into the water column at night would significantly increase horizontal advective distances. Rothlisberg (1982) found no significant differences in the day-night abundance of the early larval stages, inferring that the larvae were not going below the lowest pump inlet (within 2.5 m of bottom) during the day. The likelihood of the filter-feeding early larvae settling on the bottom, even intermittently, is remote. At later developmental stages (early postlarvae) they do become epibenthic. Therefore, potential advective distances probably fall within the range of modelled results: the smaller distances (ca. 50 km) for larvae that migrate but never rest on the bottom, and over 160 km for larvae that rest on the bottom during all daylight periods. With proximity to nearshore and estuarine nursery grounds postlarvae also shift from a diurnal, light modulated behavior pattern to a vertical migration keyed to the tides (Staples, 1980; for a review of earlier work see Garcia and Le Reste, 1981). As these late postlarvae are epibenthic, their behavior

could be influenced by a number of additional factors including current speed, pressure, salinity or environmental cues of a terrigenous origin.

The results of advecting the vertically migrating larvae can explain the large spatial and temporal patterns of postlarval *Penaeus merguiensis* immigration into the rivers of the Gulf of Carpentaria as described by Staples (1979). For the Karumba area, the October larvae are carried southward toward the Norman River whereas the March larvae are carried away from the nursery areas toward the center of the Gulf. For the area north of Weipa, the October larvae are carried south away from likely nursery areas whereas the March larvae are carried north into Staples' Area 1. Larvae released on the mid-east coast are moved parallel to the coastline in both seasons.

The advective potential results indicate that the last day that larvae should reach the Norman River in the southeast corner of the Gulf is a little after November 21. Staples (1980) found that the peak of *P. merguiensis* postlarvae entering the Norman River in 1975–76 occurred in mid-November and that immigration was low after December 1. The close agreement between the modelled results and field observations is encouraging. The precise time at dusk and dawn that the larvae leave and arrive at their daytime depth was an important parameter in the application of the advective potential predictions. Though variable because of changes in light penetration, it seems that the daily timing of migration, in relation to tidal periodicity (both seasonal and short-term), is just as important as the geographic proximity of the spawning ground to the nursery area in determining whether or not larvae will be successfully advected toward the coast. High intensity temporal sampling during dawn and dusk would add greater resolution to the advective potential predictions.

Horizontal larval diffusion[3]

Up to now we have dealt solely with the effects of advection of larvae by vertically sheared tide and wind-induced currents. In that approach we have neglected the effect of diffusion caused by two factors: turbulence of the water and variability in vertical migratory behavior of the larval population. (This latter effect is essentially shear dispersion[4].) In the marine environment other workers have shown that diffusion is not a major force affecting larval distribution (Hirano and Fujimoto, 1968; Talbot, 1977; Okubo, 1980) but it is still important to estimate how large a part diffusion plays in influencing the number of larvae that reach the nearshore and estuarine nursery areas.

Firstly considering the diffusion due to turbulence, we assume that the diffusion is horizontally isotropic and can be quantified by an empirical horizontal diffusivity constant K_H. For these conditions, the diffusion equation for the concentration of larvae (C) as a function of time t and distance r from the center of a distribution whose

3. Here we have used the definition of diffusion (common in physical oceanography) as the spreading out of the population due to a random walk-like process.

4. Dispersion refers to the spreading out of the population due to shear in the velocity field.

advection we have already evaluated, in water of constant depth is:

$$\frac{\partial C}{\partial t} = \frac{1}{r}\frac{\partial}{\partial r}\left(r K_H \frac{\partial C}{\partial K}\right). \tag{6.1}$$

If we assume K_H is independent of r and t, then the solution of 6.1 for an initial release of N_0 larvae (assuming zero larval mortality) is:

$$C(r,t) = \frac{N_0}{4\pi K_H t} \exp\left(-\frac{r^2}{4K_H t}\right). \tag{6.2}$$

While there is no universally accepted formula for K_H, theoretical and empirical studies (reviewed by Okubo, 1980) show K_H is proportional to $\ell^{4/3}$ where ℓ is the typical length scale. For a length scale of 10–50 km, K lies in the range 10–50 $m^2\ s^{-1}$. Larval mortality can only be approximated in the Gulf from estimates of fecundity and mortalities of other life history stages. Staples (personal communication) has estimated juvenile mortality in the nursery areas as 15% $week^{-1}$ and Lucas *et al.* (1979) have estimated adult natural mortality as 5% $week^{-1}$. During the short, but intensive, fishing season approximately 85% of the adult population is removed (Lucas *et al.*, 1979). Based on these mortality rates and an estimated fecundity of 2×10^5 eggs per female (Crocos, personal communication) we estimate that only 0.1% of the spawned eggs must reach the nursery areas to maintain a stable population level. As the larvae diffuse from the center of the distribution, some fraction (say 0.5) move closer to the nursery areas and the remainder move away. If we now assume all the larvae on the shoreward side reach the nursery areas then we can estimate, with the help of a re-arranged Eq. 6.2, the maximum distance, r_m, that the center of the distribution can be from the nursery area to satisfy the 0.1% survival rate; i.e.,

$$0.001 = \frac{1}{2}\int_{r_m}^{\infty} 2\pi r \exp\left(-\frac{r^2}{4K_H t}\right) dr. \tag{6.3}$$

For the published range of values of K_H, r_m lies in the range 30–90 km.

The second contribution to diffusion (or in this case shear dispersion) comes from the variable migratory behavior of the population in different light, wind and turbidity conditions. This may be as important as turbulence in diffusing the larvae but is even more difficult to quantify. One estimate of the variability would be half the advected distance realized by the various migratory schemes presented earlier. This distance is approximately 40 km parallel to the advection direction and 15 km perpendicular to this motion. This variability would increase the value of r_m by as much as a factor of 2 parallel to the advection direction and by a somewhat smaller value in the perpendicular direction.

These calculations (which are most likely upper estimates) suggest that diffusion could aid the larvae released in October in reaching their coastal nursery areas in the southeast corner (Area 3, Fig. 1), but diffusion is barely large enough to overcome the

advection away from the nursery areas in March. The same argument applies for the northern area (Area 1) but with the seasons and directions reversed. On the mid-eastern coast (Area 2), diffusion and advection will always enable larvae to reach their nursery areas and therefore year-round recruitment is possible.

Life history and reproductive strategies

Many authors have speculated on how important the proximity of spawning grounds to nursery ground would be, along with the timing of spawning, to take advantage of the appropriate currents to effect the transfer of larvae from one habitat to the next (Hjort, 1914; Istock, 1967; Efford, 1970; Dragesund, 1971). Though penaeids have a variety of life history strategies, with some totally marine and some totally estuarine, most commercially important species have a mixed life cycle with a dependence on an estuary or nearshore zone at some stage, (Kutkuhn, 1966; Gunter, 1980). These species with the mixed life cycle also suffer the greatest recorded variations in numbers. The success of the larvae in moving between the offshore and nearshore habitats could be one of the key factors in explaining the variation in numbers. Further, since the proximity of spawning is important to the success of recruitment, and therefore the perpetuation of the species, the magnitude of the larval drift may delimit the offshore extent of the adult distributions in any given location. In the Gulf of Carpentaria, the commercial abundances of adult shrimp in the genus *Penaeus,* all of which require a nearshore or estuarine nursery area, are all found within 130 km of the coast (Somers and Taylor, 1981), even though there is no apparent depth or substrate limitation that would keep them restricted to the coastal zone. The offshore limitation of the adult distribution is within the range of larval advection distances calculated in this study.

The fact that *P. merguiensis* is not finely tuned to its environment, in that it appears to waste a large amount of its reproductive output in the southeastern Gulf of Carpentaria, with most of the population spawning when conditions are not suitable for recruitment, is at first perplexing and from an evolutionary point of view apparently untenable. Though the Gulf is at a tropical latitude there is marked seasonality in air and water temperatures, rainfall, salinity, wind regimes and currents. Reproduction, as evidenced by the spawning activity and postlarval recruitment patterns is also seasonal yet there appears to be a lack of sensitivity to the environment and reproductive inefficiency. To explain this we could first consider the relative ages of the Gulf and the penaeid species therein. From the best genetic estimates available (divergence times calculated from data in Mulley and Latter, 1980) the penaeid species that inhabit the Gulf are between 1 and 6 million years old and are thought to be relatively slowly evolving because of their very low levels of genetic variation (Redfield *et al.,* 1980). Over the past 10 million years the Gulf has not been flooded continuously and only in the last 7000 years has it reached its present extent (Doutch, 1976). Therefore, the slowly evolving penaeid species may not have had enough time to adapt to this

relatively new environment, an environment somewhat atypical to the rest of its range. Alternatively, the reproductive strategy adopted by the penaeids, though apparently very demanding (e.g., demersal eggs, complex larval life history, discrete habitat requirements through the life cycle), may be so robust, by virtue of its high fecundity and planktonic larvae, that the effects of long and short term changes in the environment are damped (Roff, 1974; Strathmann, 1974).

Clearly the advection model developed here has been very useful in showing the importance of synchronization of reproductive activity with current patterns and its effect on the timing, spatial patterns, and success of recruitment of postlarvae to nursery areas. The broad implication that bears on future studies of advection and dispersion of marine organisms is the need for detailed knowledge of both the physical environment including its dynamics and larval behavior. Variables such as wind velocity, surface current velocity and larval distribution, common in correlative studies, if taken in isolation, would give misleading impressions of which factors are critical in affecting the distance and direction of larval advection. In order to assess year to year variation in the magnitude of postlarval recruitment and subsequent year-class strength, future work of this type will have to focus not only on the hydro-meteorological events at specific times in the planktonic period, but also on a number of biological factors (food availability and predation pressure) that influence mortality during the larval drift. At present there is very little information on which to accurately assess these factors in the Gulf.

While these techniques have been applied in the Gulf of Carpentaria we believe that similar procedures could be used in a number of other areas which are closed or semi-closed to outside influences and for which mathematical models of the circulation have been developed. Such areas as the North Sea and the Gulf of Mexico would be promising by building on, for example, the work of Pingree and Griffiths (1978) and Hurlburt and Thompson (1980) respectively. For studies of year to year variations in larval transport, there is a need for space and time variable winds to force any model.

Finally, this study has been a test of the advective portion of the hypothesis put forward by Hardy (1935) almost 50 years ago. He proposed that the horizontal paths of planktonic animals will vary according to the vertical migratory behavior of the animals and the differing speeds and directions of the water masses through which they migrate. The differences in horizontal distance and direction under various migratory schemes, in this study, have been considerable. Even though the vertical migratory distances are small, the planktonic period short and the currents barotropic. There is tremendous scope for development of advective models for other animals, both mero- and holoplanktonic, that have longer planktonic lives and greater vertical migratory abilities which move through a much more diverse and dramatic array of current velocities.

Acknowledgments. We would like to thank John Salini for calculating the genetic divergence times and Eugene Rhodes for a précis of the complicated geological history of the Gulf of

Carpentaria. Derek Staples provided a hypothesis to test, unpublished data and criticism of the manuscript. Bill Dall, Phil Hindley, Barry Scott, Jan Somers, Joe Wroblewski and Peter Young gave further criticism of the manuscript. Finally we would like to thank Muriel Baxter for her excellent typing of the many drafts necessitated by the differing backgrounds of the authors.

APPENDIX

Development of the three-dimensional model

As indicated in Section 2, we assume the currents are driven by the surface pressure gradient determined from the two-dimensional model of Church and Forbes (1981) and Forbes and Church (1983) and the surface wind stress. (All nonlinear terms are neglected and thus we cannot model the second-order tide-induced residual currents.) Considering the horizontal currents u and v as a complex variable $w = u + iv$, the equation for conservation of momentum (neglecting nonlinear terms and horizontal viscosity) in a right-handed orthogonal coordinate system (the z axis vertical upward and the zero level at the sea surface) is

$$\frac{\partial w}{\partial t} + ifw = q + \frac{\partial}{\partial z}\nu\frac{\partial w}{\partial z}. \tag{A1}$$

Since the largest currents are the barotropic tide and wind-induced currents, the pressure term q is only due to the surface slope; i.e.,

$$q = -\frac{1}{\rho}\frac{\partial p}{\partial x} - i\frac{1}{\rho}\frac{\partial p}{\partial y} = -g\frac{\partial \zeta}{\partial x} - ig\frac{\partial \zeta}{\partial y} \tag{A2}$$

where ζ is the sea surface elevation above $z = 0$. Surface and bottom boundary conditions are necessary to solve Eq. A1. At the surface, we used a wind stress $F(t) = F_x(t) + iF_y(t)$; i.e.,

$$\nu\frac{\partial w}{\partial z}\bigg|_{z=\zeta} = F(t) \tag{A3}$$

At the bottom $z = -h$, the velocity must equal zero and close to the bottom ν must be small (several orders of magnitude smaller than its mid-depth value). We assume there exists a thin logarithmic sublayer close to the wall and rather than model this layer explicitly we assume a linear friction law applies at the top of this layer; i.e.,

$$\nu\frac{\partial w}{\partial z}\bigg|_{z=-h_+} = bw \tag{A4}$$

where b is the linear friction coefficient and ν is given by Eq. 2.2. Tee (1979, 1982) used various models for ν above this lower boundary layer but his measurements could not determine whether any of these models were superior to the others. Accordingly, we chose the simplest solution and assumed ν was constant throughout the water column.

Following Jordon and Baker (1980), the solution of Eq. A1 (after substituting Eq. A2) is

$$\begin{aligned}\omega(z_D t) = &\sum_{n=0}^{\infty} B_n f_n(z) \int_o^t q(t-\tau)\, e^{-if\tau}\, e^{-\lambda n^\tau}\, d\tau \\ &+ \sum_{n=0}^{\infty} (if + \lambda_n)\, D_n f_n(z) \int_o^t F(t-\tau)\, e^{-if\tau}\, e^{-\lambda n^\tau}\, d\tau.\end{aligned} \tag{A5}$$

As suggested by Jordon and Baker (1980), we have already cancelled the second and third

terms which sum to zero in their solution. λ_n and $f_n(z)$ are eigenvalues and eigenfunctions of the Sturm-Louville problem

$$-\frac{d}{dz}\nu\frac{d}{dz}f_n(z) = \lambda_n f_n(z) \tag{A6}$$

with the boundary conditions A3 and A4. For constant viscosity ν in water of depth h

$$f_n(z) = \cos(\beta_n z) \tag{A7}$$

$$\lambda_n = \nu\beta_n^2 \tag{A8}$$

and

$$\nu\beta_n \sin \beta_n h = b \cos \beta_n h. \tag{A9}$$

Let $\Theta = \beta_n h$ then from Eq. A9

$$\tan \Theta = \frac{K}{\Theta} \tag{A10}$$

where $K = bh/\nu$. On substituting Eq. 2.2 for ν, and $b = k|u|$, where k is a nondimensional drag coefficient approximately equal to 2×10^{-3}, then $K \approx 1.0$. Eq. A10 is a transcendental equation that was solved graphically for $K = 0.5$, 1 and 2. B_n and D_n are (Jordon and Baker, 1980)

$$B_n = \frac{-2 \sin \beta_n H}{\sin \beta_n 4 \cos \beta_n H + \beta_n H} \tag{A11}$$

$$D_n = \frac{1}{if + \lambda_n} \frac{2\beta_n}{\sin \beta_n H \cos \beta_n H + \beta_n H}. \tag{A12}$$

We now have all the elements for the solution of Eq. A1, assuming we know the surface slope (from the two-dimensional model) and the surface wind stress. For a numerical approximation, Jordan and Baker (1980) found the first five terms of the infinite sum in Eq. A5 a sufficient approximation. Note that for large n, $D_n(if + \lambda_n)H$ converges to 2 and the second term in the solution would diverge if it were not for the exponential in the integral which ensures rapid convergence. As in Jelesnianski (1970), we wish to form a numerical approximation to the time integral in Eq. A5. We do this by assuming q and F are constant over the time interval $\Delta\tau$ at their value at the centerpoint of their interval. We also extend the integral to consider all past events by changing the upper limit in the integral from t to ∞. The systems "memory" of the time history of the surface slope and stress is governed by the exponential $e^{-\lambda n \tau}$ giving a time scale of $1/\lambda_n$. For the zero'th mode, this time scale is of order 10 hours and higher modes have smaller decay times. Eq. A5 now becomes

$$\begin{aligned} w(z,t) = &\sum_{n=0}^{\infty} B_n f_n(z) \sum_{k=0}^{\infty} q\,(t - (k + \tfrac{1}{2})\Delta\tau) \int_{k\Delta\tau}^{(k+1)\Delta\tau} e^{if\tau} e^{-\lambda_n \tau}\, d\tau \\ &+ \sum_{n=0}^{\infty} (if + \lambda_n) D_n f_n(z) \sum_{k=0}^{\infty} F(t - (k + \tfrac{1}{2})\Delta\tau) \int_{k\Delta\tau}^{(k+1)\Delta\tau} e^{-if\tau} e^{-\lambda_n \tau}\, d\tau. \end{aligned} \tag{A13}$$

If we now assume the level of turbulence stays constant through the tidal cycle, we can rearrange (A13) such that

$$w(z,t) = \sum_{n=0}^{\infty} Q_n^t + \sum_{n=0}^{\infty} F_n^t \tag{A14}$$

where

$$Q_n^t = \frac{1}{if + \lambda_n} B_n f_n(z)\, q(f - \tfrac{1}{2}\Delta\tau)\,(A_n^0 - A_n^1) + A_n^1 Q_n^{t-\Delta\tau},$$

and

$$F_n^t = D_n f_n(z)\, F(f - \tfrac{1}{2}\Delta\tau)\,(A_n^0 - A_n^1) + A_n^1 F_n^{t-\Delta\tau} \tag{A15}$$

and

$$A_n^k = e^{-(if+\lambda_n)k\Delta\tau};$$

i.e., we now have a recussion formula for evaluating w.

The sum converges rapidly and in practice the summation was truncated at $n = 5$. Decreasing this limit to 3 had negligible effect on the final result. The pressure gradients q were found with the two-dimensional model. The sea surface elevation at the four closest grid points was fitted with a bi-linear function and the surface slopes evaluated by differentiating this function. The solution used is in an Eulerian reference frame whereas a solution in a Lagrangian reference frame is desirable. Because of the slowly varying nature of the bottom bathymetry and of the solution, the difference between these two solutions is small. In the advection of the larvae, all terms were time-centered.

REFERENCES

Bakken, E. 1966. Influence of hydrographical and meteorological factors on catch and recruitment strength of the sprat stock in Western Norway. Fisk Dir. Skr. Serie Havundersokelser, *14*, 61–71.

Bousefield, E. L. 1955. Ecological control of the occurrence of barnacles in the Miramichi estuary. Bull. Natn. Mus. Con., *137*, 1–69.

Bowden, K. F., L. A. Fairbairn and P. Hughes. 1959. The distribution of shearing stresses in a tidal current. Geophys. J. R. Astr. Soc. *2*, 288–305.

Carriker, M. R. 1951. Ecological observations of the distribution of oyster larvae in New Jersey estuaries. Ecol. Monogr., *21*, 19–38.

Church, J. A. and A. M. G. Forbes. 1981. Non-linear model of tides in the Gulf of Carpentaria. Aust. J. Mar. Freshwater Res., *32*, 685–698.

—— 1983. Circulation in the Gulf of Carpentaria. Part I. Direct observations of currents in the south east corner of the Gulf of Carpentaria. Aust. J. Mar. Freshwater Res., *34*, 1–10.

Colton, J. B. and R. F. Temple. 1961. The enigma of Georges Bank spawning. Limnol. Oceanogr., *6*, 280–291.

Cresswell, G. R. 1971. Current measurements in the Gulf of Carpentaria. Rep. Div. Fish. Oceanogr. CSIRO Aust., No. 50.

Crocos, P. and J. Kerr. 1983. Maturation and spawning of the banana prawn *Penaeus merguiensis* de Man (Crustacea:Penaeidae) in the Gulf of Carpentaria, Australia. J. Exp. Mar. Biol. Ecol., *69*.

Cushing, D. H. and F. R. Harden Jones. 1968. Why do fish school? Nature, *218,* 918–920.

Doutch, H. F. 1976. The Karumba Basin, northeastern Australia and southern New Guinea. MBR J. Aust. Geol. Geophys., *1,* 131–140.

Dragesund, O. 1970. Factors influencing year-class strength of Norwegian spring spawning herring (*Clupea harengus* Linne). Fisk Dir. Skr. Serie Havundersokelser, *15,* 381–450.

—— 1971. Factors influencing year-class strength of Norwegian spring-spawning herring (*Clupea harengus* Linne), *in* Symposium on the biology and early stages and recruitment mechanisms of herring, A. Saville ed., Rapp. P.-v. Réun., *160,* 74–75.

Efford, I. E. 1970. Recruitment of sedentary marine populations as exemplified by the sand crab, *Emerita analoga* (Decapoda, Hippidae). Crustaceana, *18,* 293–308.

Eldred, B., J. Williams, G. T. Martin and E. A. Joyce Jr. 1965. Seasonal distribution of penaeid larvae and postlarvae of the Tampa Bay area, Florida. Tech. Ser. Fla. St. Bd. Conserv., *44,* 1–47.

Forbes, A. M. G. and J. A. Church. 1983. Circulation in the Gulf of Carpentaria. Part II. Residual circulation and mean sea level. Aust. J. Mar. Freshwater Res., *34,* 11–22.

Garcia, S. and L. Le Reste. 1981. Cycles vitaux, dynamique, exploitation et aménagement des stocks de crevettes penaèides côitères. F.A.O. Fish. tech. Pap. *203,* 210 pp.

Graham, J. J., S. B. Chenoweth and C. W. Davis. 1972. Abundance, distribution, movement and lengths of larval herring along the western coast of the Gulf of Maine. Fishery Bull., U.S. Fish Wildl. Serv., *70,* 307–321.

Gunter, G. 1980. Studies on estuarine-marine dependency, p. 474–487, *in* Oceanography: The Past. M. Sears and D. Merriman, eds., Springer-Verlag, N.Y., 812 pp.

Hardy, A. C. 1935. The plankton community, the whale fisheries and the hypothesis of animal exclusion. 'Discovery' Rep., *11,* 273–360.

Hart, P. J. B. 1975. The distribution and long term changes in abundance of larval *Ammodytes marinus* (Raitt) in the North Sea, p. 171–182, *in* The Early Life History of Fish, J. H. S. Blaxter ed., Springer-Verlag, Berlin, 765 pp.

Heaps, N. S. 1972. Estimation of density currents in the Liverpool Bay area of the Irish Sea. Geophys. J. R. Astr. Soc., *30,* 415–432.

Heaps, N. S. and J. E. Jones. 1981. Three-dimensional model for tides and surges with vertical eddy viscosity prescribed in two layers. II. Irish Sea with bed friction layer. Geophys. J. R. Astr. Soc., *64,* 303–320.

Hirano, T. and M. Fujimoto. 1968. Preliminary results of investigations of the Kuroshio functioning as a means of transportation and diffusion of fish eggs and larvae. Symposium on the cooperative study of the Kuroshio and adjacent regions (CSK), F.A.O. Rome.

Hjort, J. 1914. Fluctuations in the great fisheries of northern Europe viewed in the light of biological research. Rapp. P.-v. Réun., *20,* 1–228.

Hurlburt, H. E. and J. Dana Thompson. 1980. A numerical study of loop current intrusions and eddy shedding. J. Phys. Oceanogr., *10,* 1611–1651.

Istock, C. A. 1967. The evolution of complex life cycle phenomena: An ecological perspective. Evolution, *21,* 592–605.

Jelesnianski, C. 1970. Bottom stress time history in linearized equations of motion for storm surges. Mon. Weath. Rev., U.S. Dep. Agric., *98,* 462–478.

Johns, B. 1978. The modelling of tidal flow in a channel using a turbulence energy closure scheme. J. Phys. Oceanogr., *8,* 1042–1049.

Jones, A. C., D. E. Dimitriou, J. J. Ewald and J. H. Tweedy. 1970. Distribution of early developmental stages of pink shrimp *Penaeus duorarum* in Florida waters. Bull. Mar. Sci. Gulf Caribb., *20,* 634–661.

Jordan, T. F. and J. R. Baker. 1980. Vertical structure of time dependent flow dominated by friction in a well-mixed fluid. J. Phys. Oceanogr., *10,* 1091–1103.

Kamykowski, D. 1974. Possible interactions between phytoplankton and semidiurnal internal tides. J. Mar. Res., *32,* 67–89.

—— 1976. Possible interactions between plankton and semidiurnal internal tides. II. Deep thermoclines and trophic effects. J. Mar. Res., *34,* 499–509.

Kutkuhn, J. L. 1966. The role of estuaries in the development and perpetuation of commercial shrimp resources. Am. Fish Soc. Spec. Publ., *3,* 16–36.

Leendertse, J. J. 1967. Aspects of a computational model for long period water wave propagation. Memorandum RM-5294-PR, Rand Corp., Santa Monica, California.

Leendertse, J. J., R. C. Alexander and S. K. Liu. 1973. A three-dimensional model for estuaries and coastal seas: Vol. I. Principles of computation, R-1417-OWRR, The Rand Corp., New York.

Longhurst, A. R. 1976. Vertical migration, p. 116–137, *in* The Ecology of the Seas, D. H. Cushing and J. J. Walsh, eds., Blackwell Scientific Publications, Oxford, 467 pp.

Lucas, C., G. Kirkwood and I. Somers. 1979. An assessment of the stocks of the banana prawn *Penaeus merguiensis* in the Gulf of Carpentaria. Aust. J. Mar. Freshwater Res., *30,* 639–652.

Marr. J. C. 1956. The "critical period" in the early life history of marine fishes. J. Cons. Perm. Int. Explor. Mer, *21,* 160–170.

May, R. C. 1974. Larval mortality in marine fishes and the critical period concept, *in* The Early Life History of Fish, J. H. S. Blaxter, ed., Springer-Verlag, Berlin, 765 pp.

Miller, C. B. 1970. Some environmental consequences of vertical migration in marine zooplankton. Limnol. Oceanogr., *15,* 727–741.

Mock, C. R. and M. A. Murphy. 1970. Techniques for rearing penaeid shrimp from egg to postlarvae. Proc. First Ann. Workshop World Mariculture Soc., 143–156.

Mulley, J. C. and B. D. H. Latter. 1980. Genetic variation and evolutionary relationships within a group of thirteen species of penaeid prawns. Evolution, *34,* 904–916.

Newell, B. S. 1973. Hydrology of the Gulf of Carpentaria 1970–71. Tech. Pap. Div. Fish. Oceanogr. CSIRO Aust., *35,* 29 pp.

Okubo, A. 1980. Diffusion and Ecological Problems: Mathematical Models. Springer-Verlag, Berlin, 254 pp.

Parrish, R. H., C. S. Nelson and A. Bakun. 1981. Transport mechanisms and reproductive success of fishes in the California Current. Biol. Oceanogr., *1,* 175–203.

Paulik, G. J. 1973. Studies of the possible form of the stock-recruitment curve, *in* Fish Stock and Recruitment, B. B. Parrish ed., Rapp. P.-v. Réun., *164,* 302–315.

Pearcy, W. G. 1962. Ecology of an estuarine population of winter flounder *Pseudopleuronectes americanus* (Walbaum) Parts I-IV. Bull. Bingham Oceanogr. Coll., *18,* 5–78.

Penn, J. W. 1975. The influence of tidal cycles on the distribution pathway of *Penaeus latisulcatus* Kishinouye in Shark Bay, Western Australia. Aust. J. Mar. Freshwater Res., *26,* 93–102.

Phillips, B. F., P. A. Brown, D. W. Rimmer and D. D. Reid. 1979. Distribution and dispersal of the phyllosoma larvae of the western rock lobster, *Panulirus cygnus* in the south-eastern Indian Ocean. Aust. J. Mar. Freshwater Res., *30,* 773–783.

Pingree, R. D. and D. K. Griffiths. 1978. Tidal fronts on the shelf seas around the British Isles. J. Geophys. Res., *83,* 4615–4622.

Racek, A. A. 1959. Prawn investigations in eastern Australia. Res. Bull. St. Fish. N.S.W., No. 6.

Rae, K. M. 1957. A relationship between wind, plankton distribution and haddock brood strength. Bull. Mar. Ecol., *38*, 247–269.

Redfield, J. A., D. Hedgecock, K. Nelson and J. P. Salini. 1980. Low heterozygosity in tropical marine crustaceans of Australia and the trophic stability hypothesis. Mar. Biol. Lett., *1*, 303–313.

Reinecker, M. M. 1979. Tidal propagation in the Gulf of Carpentaria. Ph.D. thesis, University of Adelaide, 143 pp.

Riley, G. A. 1976. A model of plankton patchiness. Limnol. Oceanogr., *21*, 873–880.

Rochford, D. J. 1966. Some hydrographic features of the eastern Arafura Sea and the Gulf of Carpentaria in August 1964. Aust. J. Mar. Freshwater Res., *17*, 31–60.

Roff, D. A. 1974. The analysis of a population model demonstrating the importance of dispersal in a heterogeneous environment. Oecologia, *15*, 259–275.

Rothlisberg, P. C. 1982. Vertical migration and its effect on dispersal of penaeid shrimp larvae in the Gulf of Carpentaria, Australia. U.S. Fish. Bull., *80*, 541–554.

Sandifer, P. 1975. The role of pelagic larvae in recruitment of populations of adult decapod crustaceans in the York River estuary and adjacent lower Chesapeake Bay, Virginia. Estuar. Coast. Mar. Sci., *3*, 269–279.

Saville, A. 1965. Factors controlling dispersal of the pelagic stages of fish and their influence on survival. Int. Comm. Northwest Atl. Fish. Spec. Publ., *6*, 335–348.

Somers, I. F. and B. R. Taylor. 1981. Fishery statistics relating to the declared management zone of the Australian northern prawn fishery, 1968–1979. Aust. CSIRO Mar. Lab. Rep., *138*, 13 pp.

Staples, D. J. 1979. Seasonal migration patterns of postlarval and juvenile banana prawns, *Penaeus merguiensis* de Man, in the major rivers of the Gulf of Carpentaria, Australia. Aust. J. Mar. Freshwater Res., *30*, 143–157.

—— 1980. Ecology of juvenile and adolescent banana prawns, *Penaeus merguiensis*, in a mangrove estuary and adjacent offshore area of the Gulf of Carpentaria. I. Immigration and settlement of postlarvae. Aust. J. Mar. Freshwater Res., *31*, 635–652.

Strathmann, R. 1974. The spread of sibling larvae of sedentary marine invertebrates. Am. Nat., *108*, 29–44.

Sulkin, S. D., W. Van Heukelem, P. Kelly and L. Van Heukelem. 1980. The behavioral basis of larval recruitment in the crab *Callinectes sapidus* Rathbun: A laboratory investigation of ontogenetic changes in geotaxis and barokinesis. Biol. Bull., *159*, 402–417.

Talbot, J. W. 1977. The dispersal of plaice eggs and larvae in the southern bight of the North Sea. J. Cons. Perm. Int. Explor. Mer., *37*, 221–248.

Tee, Tim-Tai. 1979. The structure of three-dimensional tide-generating currents. I. Oscillating currents. J. Phys. Oceanogr., *9*, 930–944.

—— 1982. The structure of three-dimensional tide-generating currents: Experimental verification of a theoretical model. Est. Coast. Shelf. Sci., *14*, 27–48.

Temple, R. F. and C. C. Fischer. 1965. Vertical distribution of planktonic stages of penaeid shrimp. Publs. Inst. Mar. Sci. Univ. Tex., *10*, 59–67.

Walford, L. A. 1938. Effect of currents on distribution and survival of the eggs and larvae of the haddock (*Melanogrammus aeglefinus*) on Georges Bank. Bull. Bur. Fish., Wash., *49*, 1–73.

Webb, D. J. 1981. Numerical model of the tides in the Gulf of Carpentaria and the Arafura Sea. Aust. J. Mar. Freshwater Res., *32*, 31–44.

Weinstein, M. P., S. L. Weiss, R. G. Hodgson and L. R. Gerry. 1980. Retention of taxa of postlarval fishes in an intensively flushed tidal estuary, Cape Fear River, North Carolina. Fishery Bull., U.S. Fish. Wildl. Serv., *78*, 419–436.

Wickett, W. P. 1967. Ekman transport and zooplankton concentration in the North Pacific Ocean. J. Fish. Res. Bd. Can., *24,* 581–594.

Wood, L. and W. J. Hargis, 1971. Transport of bivalve larvae in a tidal estuary. Fourth Eur. Symp. Mar. Biol., 29–44.

Woodmansee, R. A. 1966. Daily vertical migration of *Lucifer.* Planktonic numbers in relation to solar and tidal cycles. Ecology, *47,* 847–850.

Woolridge, T. and T. Erasmus. 1980. Utilization of tidal currents by estuarine zooplankton. Estuar. Coast. Mar. Sci., *11,* 107–114.

Wroblewski, J. S. 1982. Interaction of currents and vertical migration in maintaining *Calanus marshallae* in the Oregon upwelling zone—a simulation. Deep-Sea Res., *29,* 665–686.

Received: *3 August, 1982;* revised: *23 February, 1983.*